PHYSICAL REVIEW B **86**, 100506(R) (2012)

Superconducting qubit in a waveguide cavity with a coherence time approaching 0.1 ms

Chad Rigetti,[1] Jay M. Gambetta,[1] Stefano Poletto,[1] B. L. T. Plourde,[2] Jerry M. Chow,[1] A. D. Córcoles,[1] John A. Smolin,[1] Seth T. Merkel,[1] J. R. Rozen,[1] George A. Keefe,[1] Mary B. Rothwell,[1] Mark B. Ketchen,[1] and M. Steffen[1]

[1]*IBM T. J. Watson Research Center, Yorktown Heights, New York 10598, USA*

[2]*Department of Physics, Syracuse University, Syracuse, New York 13244-1130, USA*

(Received 19 March 2012; published 24 September 2012)

We report a superconducting artificial atom with a coherence time of $T_2^* = 92\ \mu$s and energy relaxation time $T_1 = 70\ \mu$s. The system consists of a single Josephson junction transmon qubit on a sapphire substrate embedded in an otherwise empty copper waveguide cavity whose lowest eigenmode is dispersively coupled to the qubit transition. We attribute the factor of four increase in the coherence quality factor relative to previous reports to device modifications aimed at reducing qubit dephasing from residual cavity photons. This simple device holds promise as a robust and easily produced artificial quantum system whose intrinsic coherence properties are sufficient to allow tests of quantum error correction.

DOI: 10.1103/PhysRevB.86.100506 PACS number(s): 03.67.Pp, 03.67.Lx, 42.50.Dv, 85.25.Cp

Superconducting quantum circuits are a leading candidate technology for large-scale quantum computing. They have been used to show a violation of a Bell-type inequality,[1] implement a simple two-qubit gate favorable for scaling,[2] generate three-qubit entanglement,[3] perform a routine relevant to error correction,[4] and very recently to demonstrate a universal set of quantum gates with fidelities greater than 95%.[5] Most of these devices employ small angle-evaporated Josephson junctions as their critical nonlinear circuit components. Device designs appear architecturally consistent with the basic requirements for quantum error correction (QEC) and fault tolerance.[6] However, the construction and operation of much larger systems capable of meaningful tests of such procedures will require individual qubits and junctions with a very high degree of coherence. Current estimates for threshold error rates—and the cumulative nature of errors originating from control, measurement, and decoherence—make likely the need for quantum lifetimes *at least* 10^3 times longer than gate and measurement times,[7] corresponding to 20 to 200 μs for typical systems.

To this end, improvements in qubit lifetimes have continued for the past decade, spurred largely by clever methods of decoupling noise and loss mechanisms from the information-storing subspace and thus realizing Hamiltonians more closely resembling their idealized versions. Recently, Paik *et al.* made a breakthrough advance[8] by embedding a transmon qubit[9,10] in a superconducting waveguide cavity. Dubbed *three-dimensional circuit QED* (3D cQED), this system produced significantly enhanced qubit lifetimes of $T_1 = 25$–$60\ \mu$s and $T_2^* = 10$–$20\ \mu$s, corresponding to quality factors for dissipation and decoherence of $Q_1 \approx 1.8 \times 10^6$ and $Q_2 \approx 7 \times 10^5$, respectively.

These results lead to two important questions. First, are similar coherence properties observable using other fabrication processes, facilities, and measurement setups? Second, what is the origin of the dephasing process suppressing T_2^* well below the no-pure-dephasing limit of $2T_1$? Is it intrinsic to the junctions or to this qubit architecture? The weight and urgency of these questions is increased by implications on scaling potential: If the results are reproducible and decoherence times can be extended close to the $2T_1$ limit for observed T_1 times, this technology becomes a strong candidate for the construction of prototype processors for testing QEC without significant need of longer coherence. It would also suggest that other designs employing small angle-evaporated junctions (e.g., traditional planar integrated superconducting circuits) could potentially attain similar coherence if present performance limits can be identified and overcome.

In this Rapid Communication we report a 3D cQED device that demonstrates the basic reproducibility of Paik *et al.* and, moreover, shows that decoherence times can be extended further by taking precautions against qubit dephasing induced by fluctuations of the cavity photon number during qubit operation. With such precautions our system was observed to have $T_1 = 70\ \mu$s ($Q_1 \approx 1.8 \times 10^6$) and $T_2^* = 92\ \mu$s ($Q_2 \approx 2.5 \times 10^6$). This level of performance places our device already well within the regime where known microwave techniques should allow quantum gate fidelities exceeding those required for fault tolerance.

In the 3D cQED framework, qubits are manufactured with standard lithographic processes while the cavities, simple macroscopic resonant enclosures, are made independently with very different techniques, such as precision machining. Individual qubits and cavities are discrete components; their properties, materials, and designs may be varied independently without special effort. The large mode volumes, structural simplicity, and absence of very large aspect ratio wires or thin films make full-device electromagnetic simulation highly accessible. These properties in turn facilitate a high degree of practical control and engineerability of the qubit system and its electromagnetic environment.

In this work we exploit these and other properties of 3D cQED systems to engineer a device more robust against qubit dephasing due to the presence and fluctuations of residual photon population in the cavity.[11,12] We do this by three parallel strategies. First, we select qubit and cavity parameters to reduce the expected qubit dephasing rate per residual photon in the fundamental cavity mode. Second, we engineer the device to limit the spectral proximity of and couplings to higher modes of the cavity. We employ a symmetric cavity shape such that the next nearest mode after the fundamental that couples to the qubit is at ≈24 GHz

(20 GHz away from the qubit transition). This design minimizes the role of higher modes and makes the standard single-mode cavity approximation more robust. Third, we aim to suppress residual cavity population by following a simple rule: The thermal photon temperature of a resonant mode, be it linear or nonlinear, is bounded by the temperature of the dissipation source limiting its quality factor (Q). Typically, Q's of cQED resonators are limited by the ohmic environment external to the resonator to which the device is coupled. But it is notoriously difficult to ensure that the modes of a feed line are thermalized to very low temperatures. Rather than solving this problem directly, we instead make use of an ideal cold resistor—the interior walls of a bulk oxygen-free high thermal conductivity (OFHC) copper cavity—as the primary source of dissipation. In conjunction with the undercoupling of the cavity to the external environment, internal cavity dissipation is expected to thermalize the cavity population to the temperature of the bulk copper, which in turn is easily anchored to the lowest available temperature.

The 3D cQED sytem we report is described in the two-level, dispersive, and single-mode cavity approximations by the Hamiltonian[9,11]

$$H/\hbar = \omega_c a^\dagger a + (\chi_0|0\rangle\langle 0| + \chi_1|1\rangle\langle 1|)a^\dagger a + \omega_{01}|1\rangle\langle 1|. \quad (1)$$

The term $(\chi_0|0\rangle\langle 0| + \chi_1|1\rangle\langle 1|)a^\dagger a$ describes the shift of the cavity mode frequency due to the presence of the qubit in the particular logical state. For a transmon, without making the rotating wave approximation (i.e., keeping terms rotating at $\omega_{01} + \omega_c$; see Refs. 13–15), these two state-dependent frequencies are separated by χ, the cavity pull:

$$\frac{\chi_1 - \chi_0}{2} = -\frac{g^2 E_C}{\Delta^2 - \Delta E_C} - \frac{g^2 E_C}{(\Delta - 2\omega_{01})(\Delta + E_C - 2\omega_{01})}, \quad (2)$$

where g is the bare coupling strength, $\Delta = \omega_{01} - \omega_c$ is the cavity-qubit detuning, and $\hbar E_C = e^2/2C_\Sigma$ is the transmon charging energy with C_Σ the total qubit capacitance.[9] In the dispersive regime the cavity pull can be larger than the intrinsic linewidth of the qubit transition (note that this can occur even when $\chi < \kappa$). In such systems, fluctuations of the cavity photon number scramble the qubit frequency and place a limit on coherence. This is of course the same mechanism that allows the cavity photons to induce a projective measurement of the qubit state.[11] It can result from both thermal and coherent cavity photon populations.

We represent thermal driving of the resonator by the master equation[16]

$$\dot{\rho} = -\frac{i}{\hbar}[H,\rho] + \sum_j \kappa_j (n_{\mathrm{th}_j}\mathcal{D}[a^\dagger]\rho + n_{\mathrm{th}_j}\mathcal{D}[a]\rho + \mathcal{D}[a]\rho), \quad (3)$$

where $\mathcal{D}[\hat{L}]\rho = (2\hat{L}\rho\hat{L}^\dagger - \hat{L}^\dagger\hat{L}\rho - \rho\hat{L}^\dagger\hat{L})/2$ is the Lindblad superoperator for dissipation, κ_j is the cavity relaxation rate through source j, and $n_{\mathrm{th}_j} = 1/(e^{\hbar\omega_{01}/kT_j} - 1)$ is the thermal photon number for source j at temperature T_j. Following a similar procedure to Refs. 17 and 18 and as outlined in the Supplemental Material[24] (see also Refs. 11 and 16 therein), the thermal-induced dephasing rate at times long compared to $1/\kappa_{\mathrm{tot}}$, where κ_{tot} is the total cavity relaxation rate, is

$$\Gamma_{\mathrm{th}} = \frac{\kappa_{\mathrm{tot}}}{2}\mathrm{Re}\left[\sqrt{\left(1 + \frac{2i\chi}{\kappa_{\mathrm{tot}}}\right)^2 + \left(\frac{8i\chi n_{\mathrm{th}}^{\mathrm{eff}}}{\kappa_{\mathrm{tot}}}\right)} - 1\right]. \quad (4)$$

For large $\kappa_{\mathrm{tot}}/\chi$,[12]

$$\Gamma_{\mathrm{th}} = \frac{4\chi^2 n_{\mathrm{th}}^{\mathrm{eff}}}{\kappa_{\mathrm{tot}}}\left(n_{\mathrm{th}}^{\mathrm{eff}} + 1\right), \quad (5)$$

while it saturates to $\Gamma_{\mathrm{th}} = \kappa_{\mathrm{tot}} n_{\mathrm{th}}^{\mathrm{eff}}$ for large $\chi/\kappa_{\mathrm{tot}}$. Here $n_{\mathrm{th}}^{\mathrm{eff}} = \sum_j \kappa_j n_{\mathrm{th}_j}/\kappa_{\mathrm{tot}}$ is the effective number of thermal photons in the cavity. As we increase the decay rate to a cold source the net effect is to lower the effective temperature of the photons in the cavity.

These suggest different possible strategies to mitigate cavity photon induced dephasing: suppress fluctuations of the photon number by using very high Q cavities, effectively pushing photon shot noise to lower and lower frequencies; or, suppress the effective photon number with a cold dissipation source internal to the cavity. In the first strategy, one must ensure that the modes of the feed lines coupled to the cavity are cold at all relevant frequencies, as the cavity modes will thermalize to the same temperature. In the second, the internal cold dissipation is expected to thermalize all cavity modes. In both cases, one pays a price in effective signal to noise of the measurement, but for different reasons. The cold dissipation leads to a loss of information-carrying photons within the cavity before they can be measured; the high-Q approach requires long measurement integration and repetition times.

Here we follow the second strategy by employing the interior surfaces of an enclosure machined from bulk OFHC copper as an ideal cold resistor that appears as parallel damping of the effective cavity resonant circuit and limits its Q. The cavity, accordingly, is undercoupled to the input and output transmission lines.

The device design and experiment setup is shown in Fig. 1. Qubits are produced in a 3-inch wafer process on c-plane 330 μm thick sapphire prior to dicing into 3.2 mm × 6.7 mm chips. The cavity is formed by two halves machined from bulk OFHC copper and has in the assembled state an interior volume of $18.6 \times 15.5 \times 4.2$ mm^3 plus symmetric cylindrical perturbations ($d = 7.7$ mm; $h = 4$ mm) of the ceiling to accommodate commercial bulkhead SMA connectors through which signals are coupled in and out. The cavity is assembled and thermalized to 10 mK with brass screws, wrapped with Eccosorb foam and aluminized mylar to protect against stray radiation,[19] and covered with a Cryoperm magnetic shield.

Microwave signals are delivered to 10 mK via attenuated 0.86 mm outer diameter coaxial lines (Coax Co. SC-086/50-SCN-CN). Measurement signals exiting the cavity pass through (respectively) a 12 GHz low-pass filter (K&L 6L250) thermalized to 10 mK with a copper wire wrap; two double-junction magnetically shielded isolators (Pamtech CWJ1019K414) thermalized to 10 mK via copper plates with multiple high-pressure contact points; and a superconducting cable (Coax Co. SC-219/50-NbTi-NbTi) running uninterrupted from 10 mK to 2.8 K and thermalized at each end and at its midpoint (80 mK) with wire wrap. At 2.8 K the signal is amplified by a low-noise wideband HEMT amplifier (Caltech SN40A110) operating from 6–18 GHz with a noise

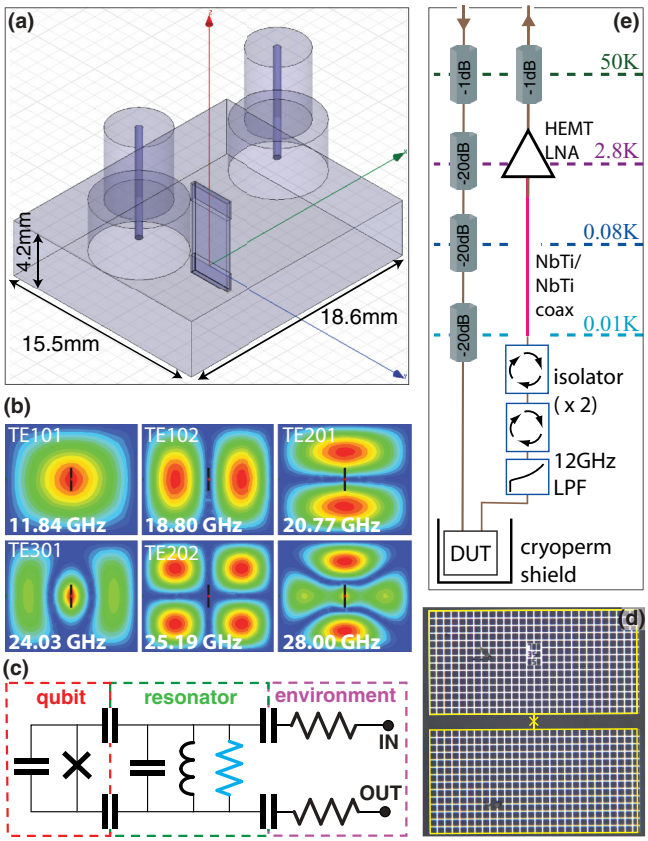

FIG. 1. (Color online) Transmon qubit in three-dimensional copper waveguide cavity with long coherence. (a) Device model (HFSS) showing interior volume of the waveguide enclosure housing a sapphire chip and transmon qubit, with two symmetric coaxial connectors for coupling signals in and out. (b) Eigenmodes of the enclosure with sapphire chip (obtained with HFSS eigenmode solver) illustrating the robustness of the single-mode-cavity approximation. The qubit is positioned at a cavity symmetry point where the electric field of the fundamental mode (TE101) is maximal. Device dimensions and symmetries imply that the next mode interacting with the qubit (TE301) is >20 GHz detuned from the qubit. (c) Equivalent circuit diagram of our device. The interior walls of the normal-metal cavity provide an ideal cold resistor (light blue) that is expected to sink the residual cavity photon population to the lowest available temperature. (d) Optical image of the transmon qubit, consisting of two capacitor pads, each 350 μm × 700 μm (outlined in yellow), and separated by a 50 μm wire interrupted by a shadow-evaporated Al/AlOx/Al Josephson junction (yellow overlay). Pads are formed of mesh with 5 μm wires and 20 μm × 20 μm holes to suppress vortex trapping and motion. (c) Cryogenic microwave measurement setup. Experiments are performed at 10 mK in a BlueFors cryogen-free dilution refrigerator.

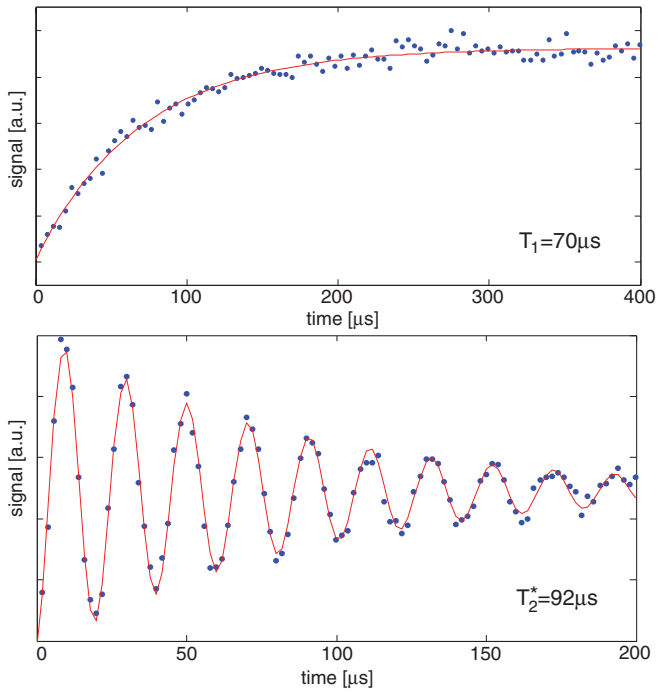

FIG. 2. (Color online) Typical quantum state lifetimes. Top: Energy relaxation time with exponential fit (red line); typical obtained times range $T_1 = 50$–70 μs. Bottom: Ramsey fringe experiment to determine coherence time with exponentially damped sinusoidal fit (red line); typical obtained times range $T_2^* = 75$–105 μs. The range of observed times is much greater than statistical fit errors.

temperature of 6 to 10 K. The signal is amplified again at room temperature, mixed down to 10 MHz, and digitized. In-phase and quadrature components are summed to produce a measurement of the qubit energy eigenstate.

With this setup we performed standard cQED (transmission) measurements to characterize the device properties and performance. The lowest resonant mode of the enclosure (TE101) is found experimentally at low power at $(\omega_c + \chi_0)/2\pi = 12.134$ GHz and at high power at $\omega_c = 12.131$ GHz.[8,20] The fundamental qubit transition is observed in spectroscopy at $f_{01} = 4.0711$ GHz. The two-photon $|0\rangle \rightarrow |2\rangle$ transition is observed 103.00 MHz below the $|0\rangle \rightarrow |1\rangle$ transition. The system is not tunable so we cannot observe a resonant interaction of the qubit and cavity but instead must infer it from observations made on the dispersively coupled system. Further, because the qubit-cavity detuning is considerably larger than the qubit frequency, the standard rotating wave approximation made in obtaining the Jaynes-Cummings Hamiltonian breaks down. Using a model without this RWA (see Supplemental Material[24]) we infer a coupling strength of $g/2\pi = 230$ MHz and a linear cavity mode shift due to the qubit logic state of $\chi/2\pi = -205$ kHz. The qubit charging energy is $E_c/2\pi = 206$ MHz corresponding to $C_\Sigma = 94.0$ fF and the Josephson junction has characteristic energy $E_J/2\pi = 10.057$ GHz implying $E_J/E_c = 49$. The cavity has a measured total quality factor of $Q = 10\,400$,[21] implying a Purcell limit on the qubit energy relaxation time of 156 μs.

Excited state lifetime and Ramsey fringe experiments yield $T_1 = 50$–70 μs and $T_2^* = 75$–105 μs (Fig. 2), where times are observed to fluctuate over minutes to hours. These data are consistent with the modes of the input and output coaxial lines having an average (blackbody) temperature of 140 mK. If the identical experiment were performed with a superconducting enclosure, the cavity modes would equilibrate to this same temperature, resulting in an effective thermal photon population for the TE101 mode of $n_{\rm th}^{\rm Al} = 0.016$ and limiting the qubit coherence time to 37 μs. Using a copper enclosure

reduces the effective temperature to 105 mK, corresponding to a TE101 population of $n_{\mathrm{th}}^{\mathrm{Cu}} = 0.004$. These results demonstrate that a highly coherent 3D cQED system is possible using a normal-metal enclosure, and further, that this provides a useful tool for the study and optimization of coherence times in cQED.

What are the trade-offs with this approach? The experimenter pays a price in convenience: The increased internal dissipation implies that for every photon exiting the cavity three are dissipated in the normal-metal walls. This places greater demands on the amplification chain to achieve a particular signal-to-noise ratio of the measurement. The availability of long coherence in cQED systems in normal-metal cavities supports the possibility for experiments where magnetic bias fields are applied from coils external to the cavity, making it possible to measure qubits requiring a flux bias and to study resonant qubit-cavity interactions in the 3D architecture.[22] An auxiliary benefit of the bulk copper cavity is the reliability of the thermal link between the qubit substrate and the fridge.

An ideal setup would employ transmission lines whose modes are already thermalized to sufficiently low temperatures. This is indeed the objective but can be challenging to realize in practice due to basic material properties at mK temperatures and the sensitivity of circuit QED systems to even small fractions of a photon.[23] Reliably achieving very low thermal number occupations is a major challenge and can be difficult to reproduce from one experimental setup to another. For this reason we have instead taken the multipronged approach described in this communication.

We have constructed a 3D qubit system based on a single-junction transmon in a copper waveguide cavity with lifetimes $T_1 = 70\ \mu$s and $T_2^* = 92\ \mu$s. Our results provide evidence that highly coherent superconducting qubits based on small shadow-evaporated Josephson junctions are reproducible with different fabrication processes and facilities. By pursuing three parallel approaches to improving coherence limits due to cavity photon induced dephasing we attained a factor of four improvement in coherence quality factor $Q_2 = 2.5 \times 10^6$ relative to previous reports. Our device falls within the range of performance required for elementary tests of error correction and fault-tolerant quantum computing procedures. We believe this performance, along with the simplicity and discrete nature of the qubits and cavities, makes this technology a strong candidate for the construction of prototype quantum processors with 10–1000 qubits.

We acknowledge discussions and contributions from Jack Rohrs, Joel Strand, Matthew Ware, and Michael DeFeo. We acknowledge support from IARPA under Contract No. W911NF-10-1-0324. All statements of fact, opinion, or conclusions contained herein are those of the authors and should not be construed as representing the official views or policies of the US Government.

[1] Markus Ansmann, H. Wang, Radoslaw C. Bialczak, Max Hofheinz, Erik Lucero, M. Neeley, A. D. O'Connell, D. Sank, M. Weides, J. Wenner, A. N. Cleland, and John M. Martinis, Nature (London) **461**, 504 (2009).

[2] J. M. Chow, A. D. Córcoles, J. M. Gambetta, C. Rigetti, B. R. Johnson, J. A. Smolin, J. R. Rozen, G. A. Keefe, M. B. Rothwell, M. B. Ketchen, and M. Steffen, Phys. Rev. Lett. **107**, 080502 (2011).

[3] L. DiCarlo, M. D. Reed, L. Sun, B. R. Johnson, J. M. Chow, J. M. Gambetta, L. Frunzio, S. M. Girvin, M. H. Devoret, and R. J. Schoelkopf. Nature (London) **467**, 574 (2010); Matthew Neeley, Radoslaw C. Bialczak, M. Lenander, E. Lucero, Matteo Mariantoni, A. D. O'Connell, D. Sank, H. Wang, M. Weides, J. Wenner, Y. Yin, T. Yamamoto, A. N. Cleland, and John M. Martinis, *ibid.* **467**, 570 (2010).

[4] M. D. Reed, L. DiCarlo, S. E. Nigg, L. Sun, L. Frunzio, S. M. Girvin, and R. J. Schoelkopf, Nature (London) **482**, 382 (2012).

[5] J. M. Chow, J. M. Gambetta, A. D. Córcoles, S. T. Merkel, J. A. Smolin, C. Rigetti, S. Poletto, G. A. Keefe, M. B. Rothwell, J. R. Rozen, M. B. Ketchen, and M. Steffen, Phys. Rev. Lett. **109**, 060501 (2012).

[6] David P. DiVincenzo, arXiv:0905.4839.

[7] Andrew W. Cross, David P. DiVincenzo, and Barbara M. Terhal, arXiv:0711.1556.

[8] Hanhee Paik, D. I. Schuster, Lev S. Bishop, G. Kirchmair, G. Catelani, A. P. Sears, B. R. Johnson, M. J. Reagor, L. Frunzio, L. I. Glazman, S. M. Girvin, M. H. Devoret, and R. J. Schoelkopf, Phys. Rev. Lett. **107**, 240501 (2011).

[9] Jens Koch, T. M. Yu, J. M. Gambetta, A. A. Houck, D. I. Schuster, J. Majer, A. Blais, M. H. Devoret, S. M. Girvin, and R. J. Schoelkopf, Phys. Rev. A **76**, 042319 (2007).

[10] J. A. Schreier, A. A. Houck, Jens Koch, D. I. Schuster, B. R. Johnson, J. M. Chow, J. M. Gambetta, J. Majer, L. Frunzio, M. H. Devoret, S. M. Girvin, and R. J. Schoelkopf, Phys. Rev. B **77**, 180502(R) (2008).

[11] J. Gambetta, A. Blais, D. I. Schuster, A. Wallraff, L. Frunzio, J. Majer, M. H. Devoret, S. M. Girvin, and R. J. Schoelkopf, Phys. Rev. A **74**, 042318 (2006).

[12] P. Bertet, I. Chiorescu, G. Burkard, K. Semba, C. J. P. M. Harmans, D. P. DiVincenzo, and J. E. Mooij, Phys. Rev. Lett. **95**, 257002 (2005).

[13] D. Zueco, G. M. Reuther, S. Kohler, and P. Hänggi, Phys. Rev. A **80**, 033846 (2009).

[14] P. Forn-Díaz, J. Lisenfeld, D. Marcos, J. J. García-Ripoll, E. Solano, C. J. P. M. Harmans, and J. E. Mooij, Phys. Rev. Lett. **105**, 237001 (2010).

[15] T. Niemczyk, F. Deppe, H. Huebl, E. P. Menzel, F. Hocke, M. J. Schwarz, J. J. Garcia-Ripoll, D. Zueco, T. Hmmer, E. Solano, A. Marx and R. Gross, Nat. Phys. **6**, 772 (2010).

[16] C. W. Gardiner and P. Zoller, *Quantum Noise: A Handbook of Markovian and Non-Markovian Quantum Stochastic Methods with Applications to Quantum Optics* (Springer, New York, 2004).

[17] M. I. Dykman and M. A. Krivoglaz, Fiz. Tverd. Tela **29**, 368 (1987) [Sov. Phys. Solid State **29**, 210 (1987)].

[18] A. A. Clerk and D. W. Utami, Phys. Rev. A **75**, 042302 (2007).

[19] A. D. Corcoles, J. M. Chow, J. M. Gambetta, C. Rigetti, J. R. Rozen, G. A. Keefe, M. Beth Rothwell, M. B. Ketchen, and M. Steffen, App. Phys. Lett. **99**, 181906 (2011).

[20] M. D. Reed, L. DiCarlo, B. R. Johnson, L. Sun, D. I. Schuster, L. Frunzio, and R. J. Schoelkopf, Phys. Rev. Lett. **105**, 173601 (2010).

[21] We also measured $Q_{\text{tot}} = 40\,000$ at the single-photon level for identical but empty (i.e., the same symmetric connector configuration; the same geometry) superconducting aluminum cavities, which we have previously shown to have internal quality factors of at least 4M. Both measurements are consistent with $Q_1 = Q_2 = 80\,000$ (the Q due to connectors 1 and 2) and for the copper cavity $Q_{\text{internal}} = 14\,000$.

[22] N. A. Masluk *et al.*, APS March Meeting 2012 Volume 57, Number 1, Q30.00002.

[23] A very recent study of qubit dephasing due to photon number fluctuations was carried out by A. P. Sears *et al.*, arXiv:1206.1265.

[24] See Supplemental Material at http://link.aps.org/supplemental/10.1103/PhysRevB.86.100506 for outline and model.